Supplementary Information: the CAM-MLM model

1. The four components of the CAM-MLM model

a. Atmosphere, land and ice components

The model atmosphere is the second version of the Community Atmosphere Model (CAM2.1), primarily developed at the National Center for Atmospheric Research (NCAR). The AGCM dynamics is based upon an eulerian spectral scheme solved on a Gaussian grid of about 2.8^o x 2.8^o latitude-longitude corresponding to a triangular horizontal truncation at 42 wave numbers. The vertical resolution is discretized over 26 levels using a progressive vertical hybrid coordinate. The reader is invited to refer to Kiehl and Gent (2004) for a detailed description of the model physics package and for its performance.

The land surface and the sea-ice components are the Community Land Model (CLM2, Oleson et al 2004) and the Community Sea-Ice Model (CSIM, Briegleb et al 2004), respectively. The dynamical core of the latter has been turned off in the present case.

b. Ocean components

The ocean component (hereafter MLM) consists of single independent column models with explicit mixed layer physics and no horizontal advection. MLM is based on Gaspar (1988)'s formulation as implemented by Alexander and Deser (1995). In the present study, we use a modified version of that used in Alexander et al (2000) where we have first included additional layers at the bottom of the ocean now reaching 1500 m or the actual depth which ever is shallower, and where we have implemented the coupling between the thermodynamical sea-ice component of CSIM and the MLM surface layer. Each ocean point has 36 vertical levels with 15 layers in the upper 100m and a realistic bathymetry (Fig. SI1). Very shallow areas (< 40 m) are treated as a fixed 50m-depth slab ocean. Others have a varying mixed layer depth (h or MLD) computed as a prognostic variable W_e (vertical entrainment rate) based on turbulent kinetic energy parameterization when deepening (Eq. SI1)

$$\frac{dh}{dt} = W_e = f\,(M + B - \frac{D}{\Delta\rho - S}) \quad \text{(Eq. SI1)}$$

where *M* is the mechanical turbulence and is function of u_* the friction velocity, *B* the buoyancy forcing which is function of the net surface heat flux Q_{net} and the net water flux *(E-P)* with *E* the evaporation and *P* the precipitation, *D* the dissipation term, $\Delta\rho$ the density jump at base of the mixed layer, and *S* the wind induced shear across the mixed layer.

When shoaling, *h* is a diagnostic quantity based on the balance between wind stirring and net surface buoyancy forcing over the depth of the mixed layer (Eq. SI2):

$$W_e = 0 \text{ and } h = f\left(\frac{M}{B-D}\right) \quad \text{(Eq. SI2)}$$

The MLD is not forced to coincide with the levels of the layered model but is constrained to be greater than 19 m and less than 1350 m or the bottom of the ocean when reached.

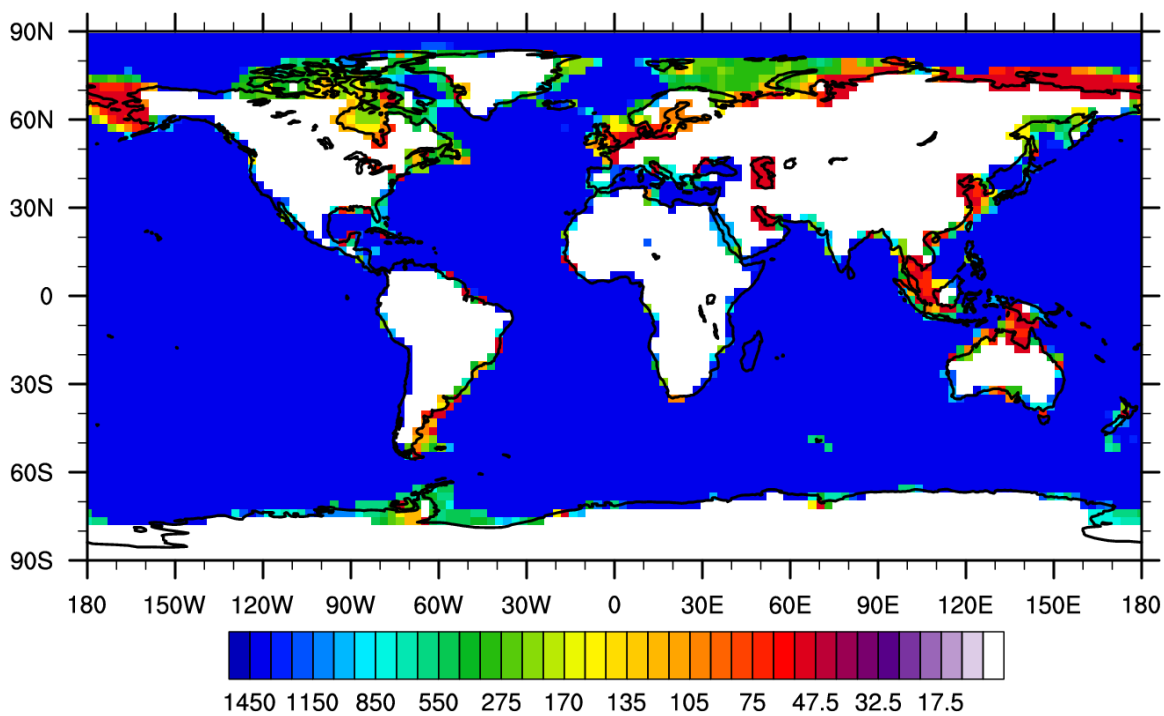

Fig.SI1: Bathymetry of the MLM model (meters)

The temperature (T_{ML}=SST) and salinity (S_{ML}=SSS) tendency of the mixed layer for open ocean grid points is given by Eq. 3, respectively,

$$\frac{\delta T_{ML}}{\delta t} = \frac{(Q_{net} + Q_{cor} - Q_{swh})}{\rho_o C_p h} + \frac{W_e(T_{ML} - T_b)}{h} + CA + \frac{\kappa_h}{h}\frac{\delta T_{ML}}{\delta z}\Big|_{z=h}$$

(Eq. 3)

$$\frac{\delta S_{ML}}{\delta t} = \frac{S_{ML}(E - P) + S_{cor}}{\rho_o h} + \frac{W_e(S_{ML} - S_b)}{h} + \frac{\kappa_s}{h}\frac{\delta S_{ML}}{\delta z}\Big|_{z=h}$$

where ρ_o is the density of seawater, C_p the specific heat of ocean water, W_e is the entrainment rate, T_b and S_b are respectively the temperature and salinity at the model level just below h, Q_{swh} is the penetrating solar radiation at h, Q_{net} is the net surface energy flux into the ocean and E-P is the net water flux. CA stands for convective adjustment occurring when the mixed layer is denser than the layer below. κ_h and κ_s are the vertical eddy diffusivity coefficient accounting for small-scale motions and are equal to 9yr^{-1} and 4yr^{-1}, respectively. Q_{swh} is calculated up to a depth of 300 meters and is prescribed following Paulson and Simpson (1977). 5 different types of water with different optical properties are taken into account as shown in Fig. SI2.

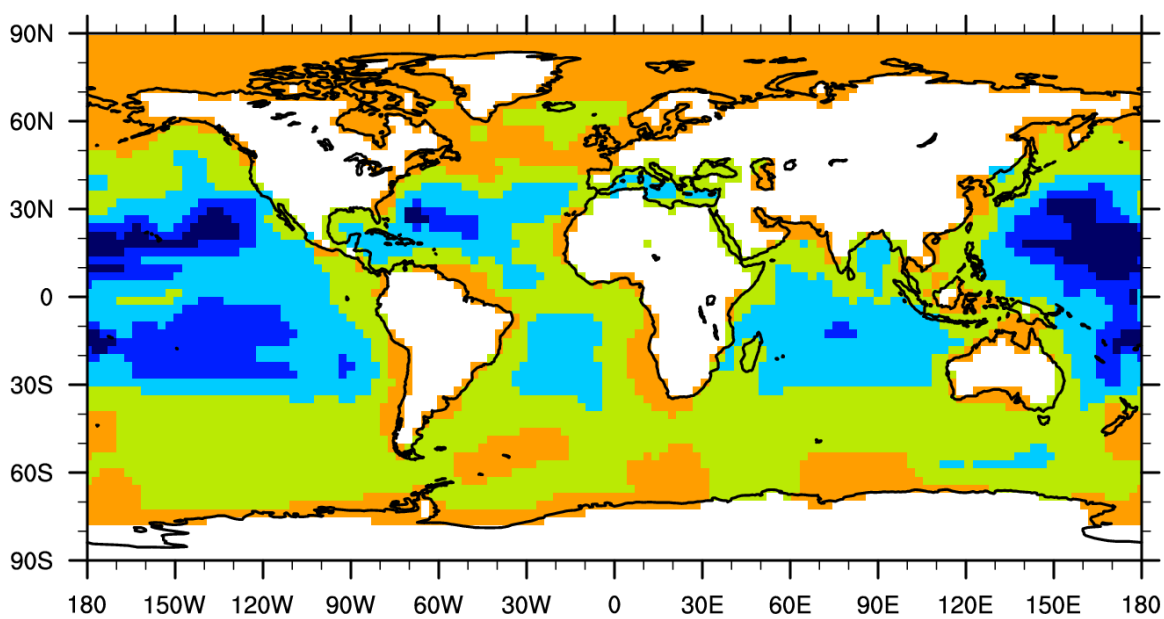

Fig.S21: 5 Ocean color types in the MLM model

c. *Coupling*

Land, sea-ice and ocean models are aligned with the CAM grid. Coupling between the ocean and the other components occurs daily, while the atmosphere, ice and land modules exchange flux and mass quantities at the CAM time step (20 minutes).

2. Surface flux correction terms

To prevent the modeled climate system from drifting far away from the observed mean state, additional flux correction terms (Q_{cor} and S_{cor}, respectively) have to be included in the computation of temperature and salinity tendency equations. Those terms compensate for all the missing physics in the ocean such as heat and salinity transport by the mean currents, diffusion etc. Q_{cor} and S_{cor} should not be compared to the so-called "flux correction approach in Coupled Global Circulation Models" which are applied to *adjust* the mean climate state of the model. In our case, the correction terms are mandatory to *simulate* a realistic climate state. They are several orders of magnitude higher and mostly preserve the observed ratio between atmospheric and oceanic heat transport.

Q_{cor} and S_{cor} are obtained from a stand-alone integration of MLM driven by daily surface fluxes from a preliminary [CAM+CSIM] uncoupled simulation forced by observed HadiSST SST and sea-ice extent over 1950-1999 (Rayner et al 2003). For a given day (d), Q_{cor}(d) is computed from the departure between the *modeled* SST(d+1) value given by MLM driven by CAM surface fluxes(d) and the *observed* SST(d+1) value. In other words, it corresponds to the energy term necessary for MLM to realistically reproduce the observed daily SST variation. As described previously, the departure between observed and modeled SST is mostly explained by the missing of ocean advection but also by intrinsic errors of CAM surface fluxes. A similar setup is used to compute S_{cor} based on the Levitus long-term mean dataset of surface salinity (SSS) (Monterey and Levitus 1997).

When ice occurs, two additional terms given by CSIM are added in the Q_{cor} formulation (daily sea-ice extent estimated from HadiSST are imposed in a forced mode and CSIM only calculates fluxes associated with ice changes). They correspond to the conductive heat flux at the bottom of the ice layer that is passed to the ocean, and to the latent heat of fusion due to ice volume changes. Those two terms are weighted by the observed sea-ice fraction. A similar setup is applied for S_{cor} under ice. In that case, the additional terms correspond to the water budget on the surface ice and to the fresh water flux due to ice volume change, both converted into equivalent salt flux weighted by the observed sea ice fraction. The brine rejection when ice is forming is also computed in CSIM and is included in the latter term.

Q_{cor} and S_{cor} climatologies including both CAM and CSIM fluxes contributions are then obtained daily from the 50-yr integration average. The December-February (DJF) and June-August (JJA) Q_{cor} values are shown in Fig. SI3. Heat is mainly added in the winter hemisphere oceans while it is extracted year-round in a 10°N-10°S latitudinal band especially in the tropical Pacific and tropical Atlantic. The latter compensates for the missing horizontal ocean advection along the equatorial cold tongues and for their associated upwelling. The former compensates in DJF and in the northern hemisphere, for the missing heat meridional advection along the Gulf Stream and its North Atlantic extension, as well as along the Kuroshio Current in the Pacific (Fig. SI3a). In JJA and in the southern hemisphere, austral winter Q_{cor} brings heat along the storm track into the mixed layer, which is fed in nature by intrusions of warm intermediate waters that are not simulated in MLM (Fig. SI3b).

In boreal summer, the heat transport by the western boundary currents in the northern hemisphere is considerably reduced, but for the Labrador Current whose cooling action on the atmosphere is strongest (Fig. SI3b). In fact, summer Q_{cor} mostly accounts for both atmospheric and MLM model errors. In the northern hemisphere, overestimated JJA trade-winds in stand-alone CAM in both the Pacific and Atlantic basins tend to overcool the subtropical surface ocean and are compensated by a positive Q_{cor} between 10°N and 45°N (Fig. SI3b). On the ocean model side, the stand-alone MLM tends to create a too deep mixed layer in these areas mostly because of the frequency of coupling between the oceanic and atmospheric models. In the southern hemisphere, austral summer Q_{cor} mostly cools down the extratropical upper ocean (Fig. SI3a). Such a sign is explained by the stand-alone MLM tendency to systematically produce too-shallow mixed layer in summertime at midlatitudes (see also in the northern Atlantic in JJA [40°-70°N], Fig. SI3b).

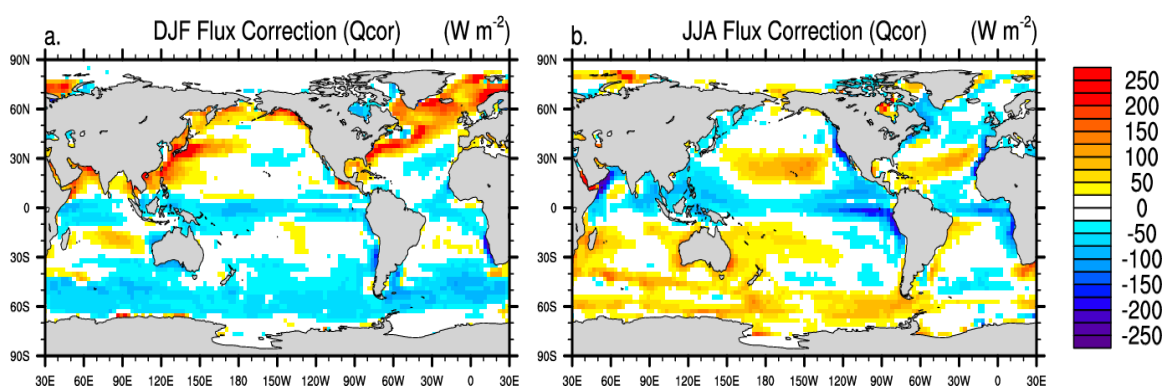

*Fig.SI3: DJF **(a)** and JJA **(b)** average surface heat flux correction (W m^2). Positive values indicate heat is added to the ocean. Shading interval is 25 W m^2.*

3. Coupled mean state

We performed a 150-yr coupled integration hereafter referred to as CTL where Q_{cor} and S_{cor} flux correction terms are applied. The initial ocean state is derived from the mean three-dimensional conditions of the off-line MLM simulation used to compute the daily climatology of Q_{cor} and S_{cor}. The coupled model reproduces rather well the SST mean state and differences between CTL and observed SST climatologies are weak as shown in Fig. SI4. Year-round tropical and midlatitude winter SSTs are very well simulated (within +/-0.3^{o}C bias); the largest errors occur in the extratropical summer oceans. The latter are overly warm due to shallower-than-observed MLD. Maximum amplitude locally peaks at +1.2^{o}C in the southern hemisphere for DJF within a 30°-50°S band (Fig. SI4a). A bias of ~ +1°C is found basin-wide in the North Pacific and North Atlantic extratropical oceans in JJA (Fig. SI4b). Despite Q_{cor}, it appears that the stand-alone model systematic errors are not totally compensated by the flux correction terms in coupled mode. In winter, the strongest bias (~+1°C) occurs in the Labrador Sea along the Labrador Current (Fig. SI4a). It is attributed to the crude representation of ice and salinity related processes (dynamics in particular) that control a large part of the ocean vertical profiles in these regions.

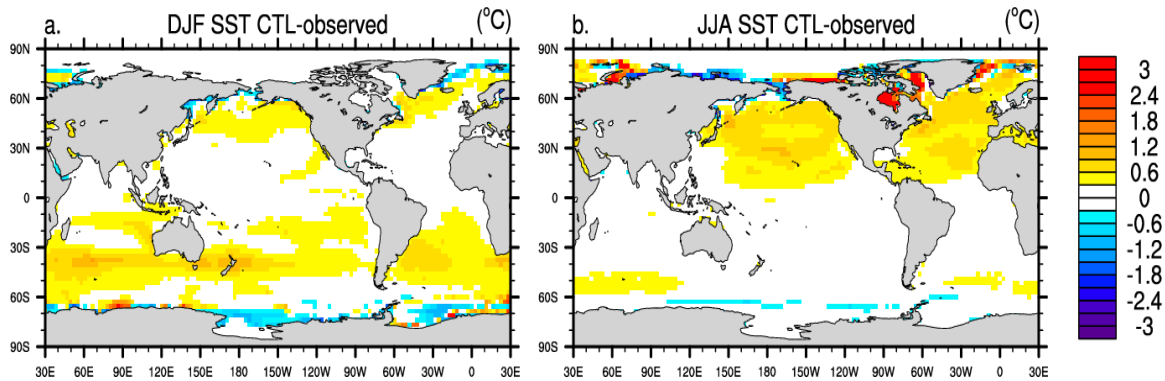

*Fig.SI4: CTL mean SST bias (^{o}C) for DJF **(a)** and JJA **(b)** average given by the difference between the 150-yr mean climatology of CTL SST and the climatology of HadiSST SST over 1950-1999. The latter period corresponds to the one used to force CAM whose daily surface fluxes were then subsequently used to compute the CTL flux correction terms. Shading interval is 0.3^{o}C*

Most of the significant SST biases occur along the ice edge especially in boreal summer (Fig. SI4b). The arctic domain covered by ice in JJA is too shrunk compared to observations (Fig. SI5b). Earlier and overestimated melting of sea-ice in spring in the Hudson Bay and in the subarctic basins (Labrador, Greenland and Kara Seas) is associated with significantly too warm SSTs in JJA while the Laptev and the East Siberian Seas are significantly too cold due to delayed melting (Fig. SI4b). In winter, the simulated sea-ice matches very well the estimated observed extent (Fig. SI5a). Marginal errors are found along the Greenland Sea ice tongue that is slightly too broad and in the Labrador Sea

where the winter sea-ice does not penetrate enough southeastward, consistently with the warmer SST.

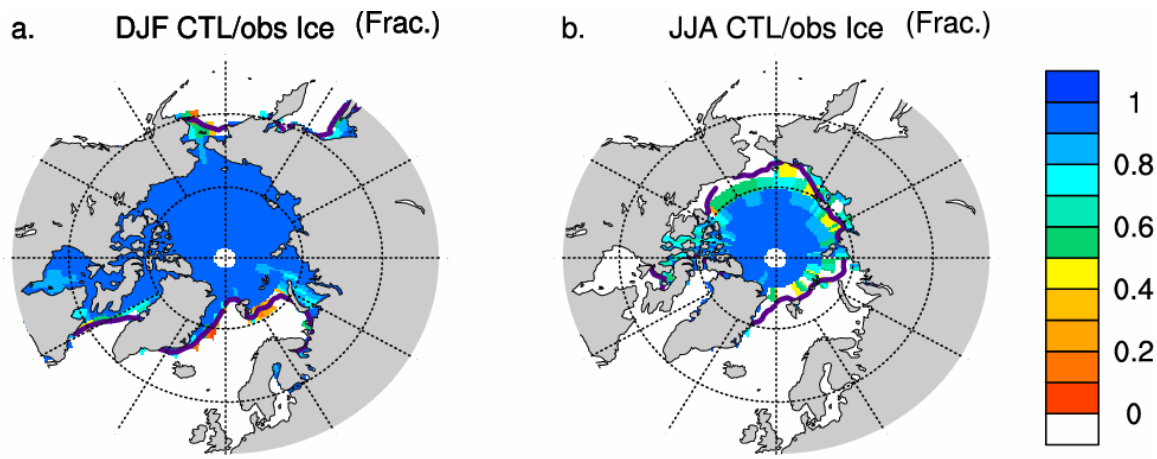

*Fig.SI5: 150-yr climatology of simulated sea ice fraction for CTL (shading), for DJF **(a)** and JJA **(b)** average. The 0.5 limit for the HadiSST sea ice climatology is superimposed (purple thick line). Shading interval is 0.1.*

In the southern hemisphere, biases are minor for sea-ice (Fig. SI6) especially in winter. In summer the melting in the Ross and Weddell seas is underestimated. Note here that the implementation of the fresh water/salinity flux exchanges between the ocean and ice model components appeared crucial in both controlling the wintertime sea-ice spatial growth and initiating the summertime melting. For the latter, it significantly shoals the ocean mixed layer, then allowing for rapid warming of open-waters. For the former, the brine rejection term that dominates, deepens the ocean mixed layer and delays its rapid cooling. Note also that in the course of the coupled simulation, Q_{cor} is set to zero when negative (*i.e.* when it tends to cool down the SST) when the entire ocean surface is covered by ice. The latter correction is necessary and physically justified to have a reasonable seasonal cycle of the sea-ice extent especially during the spring and summer melting seasons.

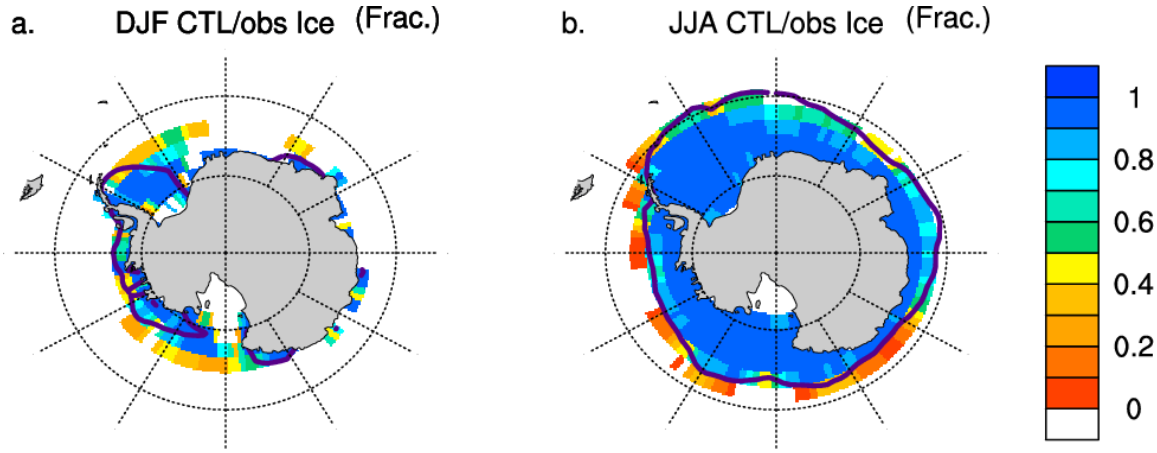

Fig.SI6: Same as Fig.SI5 but for the southern hemisphere

The maximum simulated MLD is shown in Fig. SI7 for boreal winter and summer seasons, respectively. As in observations (see, de Boyer Montegut et al 2004 for instance), the deepest MLD occurs in the winter hemisphere. In the northern hemisphere, maxima follow the vigorous storm tracks both in the North Pacific and in the North Atlantic with simulated values between 150-200 meters (Fig. SI7a). Greater depths are found between Greenland and Great Britain as well as in the Labrador and Norwegian Sea. They correspond to deep water formation controlled by complex convective processes leading locally to instantaneous values as high as 1500 m in the observations (Dickson et al 1996). In CTL, even if some grid points around Iceland and Spitzberg reach 600-700 meters, the north Atlantic MLD is clearly underestimated with mean simulated values around 250m. Such a weak magnitude is very common for this type of model and the reader is invited to refer to as Alexander et al (2000) for a list of factors that may contribute to such a model behavior.

Within the subtropical band, as stated previously, MLM tends to produce a too deep MLD in the trade wind regions in winter with values as high as 120 m instead of 50-70m estimated in the observations (Fig. SI7a). Such a bias is persistent in summer especially in the Pacific and Atlantic between 10°N and 30°N where the MLD is twice too deep (Fig. SI7b).

Realistic mixed layer deepening is found along the austral winter storm track.

Note finally that there is no significant drift in the coupled model over open water in MLD, temperature and salinity. However a clear trend in salinity is found under permanent sea-ice points.

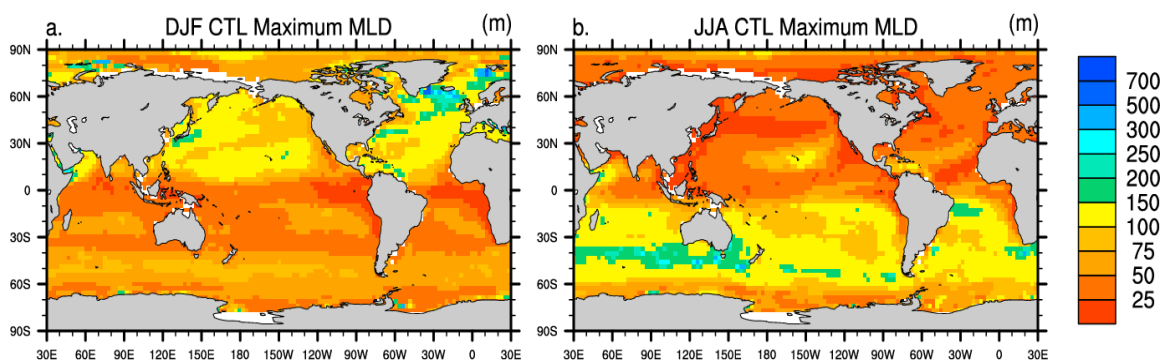

*Fig.SI7: Simulated maximum mixed layer depth (m) for boreal **(a)** and austral **(b)** winter. Note that the shading interval changes with depth: 25m for h<100, 50m for 100<h<300, and 200m for deeper h.*

References

Alexander, M. A., and C. Deser, 1995: A mechanism for the recurrence of wintertime midlatitude SST anomalies. *J. Phys. Oceanogr.*, **25**, 122-137.

Alexander, M. A., J. D. Scott, and C. Deser, 2000: Processes that influence sea surface temperature and ocean mixed layer depth variability in a coupled model. *J. Geophys. Res.*, **105**, 16823-16842.

Briegleb, B. P., C. M. Blitz, E. C. Hunke, W. H. Lipscomb, M. M. Holland, J. L. Schramm, and R. E. Moritz, 2004: Scientific description of the sea ice component in the Community Climate System Model, Version 3. NCAR Tech. Note NCAR/TN463+STR, 70pp.

Dickson, R. R., J. Lazier, J. Meincke, P. Rhines, and J. Swift, 1996: Long term coordinated changes in the convective activity of the North Atlantic. *Prog. Oceanogr.*, **38**, 241-295.

Gaspar, P., 1988: Modeling the seasonal cycle of the upper ocean. *J. Phys. Oceanogr.*, **18**, 161-180.

Kiehl, J. T., and P. R. Gent, 2004: The community climate system model, version 2. *J. Climate*, **17**, 3666-3682.

Oleson, K. W., and co-authors, 2004: Technical description of the Community Land Model (CLM). NCAR Tech. Note NCAR/TN-461+STR, 174pp.

Paulson, C. A., and J. J. Simpson, 1977: Irradiance measurements in the upper ocean, *J. Phys. Oceanogr.*, ***7***, 952-956.

Rayner, N.A., E.C. Kent, and A. Kaplan, 2003: Global analyses of sea surface temperature, sea ice, and night marine air temperature since the late nineteenth century*. J. Geophys. Res.,* **108**, 4407, doi:10.1029/2002_JD002670.